



# Preconditioning the Helmholtz Equation for Rigid Ducts

Kenneth J. Baumeister  
Lewis Research Center, Cleveland, Ohio

Kevin L. Kreider  
University of Akron, Akron, Ohio

National Aeronautics and  
Space Administration

Lewis Research Center

Available from

NASA Center for Aerospace Information  
800 Elkridge Landing Road  
Linthicum Heights, MD 21090-2934  
Price Code: A03

National Technical Information Service  
5287 Port Royal Road  
Springfield, VA 22100  
Price Code: A03

# PRECONDITIONING THE HELMHOLTZ EQUATION FOR RIGID DUCTS

**Kenneth J. Baumeister**

National Aeronautics and Space Administration  
Lewis Research Center  
Cleveland, Ohio 44135

**Kevin L. Kreider**

The University of Akron  
Department of Mathematical Sciences  
Akron, Ohio 44325-4002

## ABSTRACT

An innovative hyperbolic preconditioning technique is developed for the numerical solution of the Helmholtz equation which governs acoustic propagation in ducts. Two pseudo-time parameters are used to produce an explicit iterative finite difference scheme. This scheme eliminates the large matrix storage requirements normally associated with numerical solutions to the Helmholtz equation. The solution procedure is very fast when compared to other transient and steady methods. Optimization and an error analysis of the preconditioning factors are present. For validation, the method is applied to sound propagation in a 2D semi-infinite hard wall duct.

## INTRODUCTION

The Helmholtz equation plays an important role in the study of acoustics as well as electromagnetic propagation and quantum mechanics. Unfortunately, large matrix storage requirements are generally associated with numerical solutions of the Helmholtz equation. To reduce these requirements, Bayless, Goldstein, and Turkel (1982) developed an iterative approach to solve the associated matrix equation. More recently, Baumeister and Kreider (1996) developed a preconditioned transient finite difference scheme to solve the Helmholtz equation as well as the more general linearized potential flow equations. Their introduction of time dependence into the Helmholtz equation eliminates the large matrix storage requirements of the algorithm. This paper is concerned with the development of a more efficient preconditioning method to accelerate convergence for the Helmholtz equation.

A standard technique of solving steady state partial differential equations is to march their time dependent form until the steady state is reached. When the transient is not of interest, acceleration parameters can be employed to speed the convergence. This type of differential manipulation is often associated with preconditioning of both time dependent (Turkel, Fiterman and van Leer, 1993) and time independent (Turkel and Arnone, 1993) partial differential equations. Generally, acceleration parameters destroy the time accuracy of the solution. Turkel (1982, pp. 31)

addresses many of the issues associated with the acceleration to a steady state solution.

In this paper, new preconditioning factors are introduced to speed the convergence of the transient finite difference scheme in solving the Helmholtz equation. Solution times are reduced by an order of magnitude over the previous approach. For validation, the method is applied to plane wave sound propagation in a 2D semi-infinite hard wall duct. The paper contains a description of the problem, the brief development of the preconditioning technique, the introduction of the acceleration parameters, the finite difference formulation with a stability analysis, and several numerical examples with error estimates.

## NOMENCLATURE

- $C_o^\#$  dimensional speed of sound
- $C$  dimensionless speed of sound, Eq. (2)
- $D^\#$  dimensional duct height
- $D$  duct height,  $D^\#/D^\#$ ,  $D = 1$
- $e_k$  total  $L_1$  convergence error at step  $k$ , Eq. (16)
- $e_{k\lambda}$   $e_k$  error per axial wavelength, Eq. (17)
- $f^\#$  dimensional frequency
- $f$  dimensionless frequency,  $f^\#D^\#/C_o^\#$ , Eq. (2)
- $i$   $\sqrt{-1}$
- $L$  length,  $L^\#/D^\#$
- $|M|$  absolute value of Mach number, Eq. (12)

- n unit outward normal
- t dimensionless time,  $f^{\#}t^{\#}$
- $t_T$  dimensionless total calculation time
- $\Delta t$  time step
- x dimensionless axial coordinate,  $x^{\#}/D^{\#}$
- $\Delta x$  axial grid spacing
- y dimensionless transverse coordinate,  $y^{\#}/D^{\#}$
- $\Delta y$  transverse grid spacing
- $\alpha$  acceleration parameter
- $\beta$  acceleration parameter
- $\phi'$  transient potential,  $\phi^{\#}/C_o^{\#}D^{\#}$  Eq. (1)
- $\phi$  transient potential in frequency domain, Eq. (6)
- $\psi$  Fourier transformed potential, Eq. (3)
- $\omega$  dimensionless frequency,  $2\pi f$

**Subscripts**

- i axial index, see Fig. 1
- j transverse index, see Fig. 1
- o ambient or reference condition

**Superscript**

- # dimensional quantity
- k time step
- complex conjugate

**PROBLEM STATEMENT**

The problem under consideration here is the development of preconditioning acceleration factors to obtain the solution to the Helmholtz equation. This method will have application to the general study of sound propagation in ducts. The goal of the paper is to develop a stable, explicit finite difference scheme that significantly reduces the computation time required to solve the Helmholtz equation with a monochromatic noise source. The formulation is applied to a semi-infinite duct with a planar source at the duct inlet, as shown in Fig. 1.

**HELMHOLTZ EQUATION AND BOUNDARY CONDITION**

The governing differential equation for studying wave propagation can be formulated in terms of a potential as

$$\frac{1}{C^2} \phi'_{tt} = \phi'_{xx} + \phi'_{yy} \quad \text{or} \quad f^2 \phi'_{tt} = \phi'_{xx} + \phi'_{yy} \quad (1)$$

where  $\phi'(x,y,t)$  is the dimensionless potential and subscripts indicate partial differentiation with respect to subscripted variables. The conventional normalization factors used to develop these nondimensional equations are given in the NOMENCLATURE. The dimensionless frequency  $f$  is defined as

$$f = \frac{f^{\#}D^{\#}}{C_o^{\#}} = \frac{1}{C} \quad (2)$$

where the superscript # indicates a dimensional quantity.

There are several ways to develop a frequency domain formulation for Eq. (1). The Fourier Transform can be applied if the potential has a multi-frequency content. In the monochromatic case, this is equivalent to assuming that

$$\phi'(x, y, t) = \psi(x, y)e^{-i\omega^{\#}t^{\#}} = \psi(x, y)e^{-i2\pi t} \quad (3)$$

which transforms Eq. (1) to the Helmholtz equation

$$0 = \psi_{xx} + \psi_{yy} + \omega^2 \psi \quad (4)$$

where  $\omega = 2\pi f$ .

At the entrance of the duct,  $x = 0$ , the source is assumed to have the form

$$\phi' = e^{-i2\pi t} \quad \text{or} \quad \Psi = 1 \quad (5)$$

Also, the duct is assumed to be semi-infinite in length so that waves propagate only to the right.

**PRECONDITIONED HELMHOLTZ EQUATION**

The Helmholtz equation is preconditioned by assuming that

$$\phi'(x, y, t) = \phi(x, y, t)e^{-i\omega^{\#}t^{\#}} = \phi(x, y, t)e^{-i2\pi t} \quad (6)$$

See Baumeister and Kreider (1996) for further discussion. This differs from the classical monochromatic transformation in that the amplitude  $\phi$  (no prime) is no longer independent of time. Under this transformation, Eq. (1) becomes

$$f^2 \phi_{tt} - 2if\omega \phi_t = \phi_{xx} + \phi_{yy} + \omega^2 \phi \quad (7)$$

The only difference between the Helmholtz Eqs. (4) and (7) is the presence of the time derivative terms on the left hand side. Physically, the time dependence in  $\phi(x,y,t)$  is caused by assuming that the duct is quiescent at time 0, and that the source is turned on at that instant. A series of numerical calculations reported by Baumeister and Kreider (1996) show that

$$\lim_{t \rightarrow \infty} \phi(x, y, t) = \psi(x, y) \quad (8)$$

when the  $f^2\phi_{tt}$  is dropped (parabolic approximation).

### ACCELERATION PARAMETERS

To speed the convergence to the steady state solution  $\psi(x,y)$ , acceleration parameters  $\alpha$  and  $\beta$  are added to Eq. (7) as follows:

$$\alpha f^2 \phi_{tt} - \beta 2if\omega\phi_t = \phi_{xx} + \phi_{yy} + \omega^2\phi \quad (9)$$

This is a generalization of the preconditioning done in Baumeister and Kreider (1996), which dealt with the  $\alpha = 0, \beta = 1$  case (parabolic approximation). After the formulation of the difference equations, the acceleration of convergence is tested over a range of acceleration parameters.

### FINITE DIFFERENCE EQUATIONS

The potential at the spatial grid points  $(x_i, y_j)$  (Fig. 1) is determined by iterating the initial condition over time steps  $t^k = k\Delta t$ . Away from the duct boundaries, each partial derivative in Eq. (9) can be expressed using central differences, which yields

$$\begin{aligned} \phi_{i,j}^{k+1} \left( \frac{\alpha f^2}{\Delta t^2} - \frac{\beta i\omega f}{\Delta t} \right) &= \phi_{i,j}^k \left( \frac{2\alpha f^2}{\Delta t^2} - \frac{2}{\Delta x^2} - \frac{2}{\Delta y^2} + \omega^2 \right) \\ &+ \phi_{i+1,j}^k \left( \frac{1}{\Delta x^2} \right) + \phi_{i-1,j}^k \left( \frac{1}{\Delta x^2} \right) \\ &+ \phi_{i,j+1}^k \left( \frac{1}{\Delta y^2} \right) + \phi_{i,j-1}^k \left( \frac{1}{\Delta y^2} \right) \\ &+ \phi_{i,j}^{k-1} \left( -\frac{\alpha f^2}{\Delta t^2} - \frac{\beta i\omega f}{\Delta t} \right) \end{aligned} \quad (10)$$

where  $\Delta x, \Delta y,$  and  $\Delta t$  are the space and time mesh spacings respectively, and  $\phi_{ij}^k = \phi(x_i, y_j, t^k)$ . Equation (10) is an explicit two step scheme. The field values at  $t^0$  and  $t^{-1}$  are assumed zero because the initial field is quiescent.

The expressions for the difference equations at the hard wall boundaries ( $y=0$  &  $y = 1$ ) employ the boundary condition

$$\nabla\phi \cdot \mathbf{n} = 0 \quad (11)$$

where  $\mathbf{n}$  is the unit outward normal. Baumeister (1980) gives precise details for generating the difference equations on the boundaries.

### STABILITY

A von Neumann stability analysis is used to determine the conditions on  $\Delta t, \Delta x,$  and  $\Delta y$  required for conditional stability as a function of the acceleration parameters  $\alpha$  and  $\beta$ . Conditional stability means that the amplification factor, which describes how errors propagate from one time step to the next, has magnitude one. Thus, when  $\Delta t, \Delta x,$  and  $\Delta y$  satisfy the stability criteria, errors are not magnified or diminished in magnitude. This is a desirable property, since the numerical formulation cannot distinguish between a roundoff error and a small physical oscillation.

For the case  $\alpha = 0$  and  $\beta = 1$ , treated by Baumeister and Kreider (1996) and herein denoted the parabolic preconditioner (because the second order time derivative does not appear), the stability analysis indicates that the method is conditionally stable, subject to the condition (conservative estimate of Mach number effects)

$$\Delta t < \frac{1}{\omega f \left[ \left( \frac{1}{\Delta x} \right)^2 + \left( \frac{1}{\Delta y} \right)^2 \right] - \pi + \frac{|M|}{f\Delta x}} \quad (12)$$

In a typical application,  $f$  is set by the operating conditions in the duct. The grid spacing parameters  $\Delta x$  and  $\Delta y$  are set to resolve the estimated spatial harmonic variation of the potential field and  $\Delta t$  is chosen to satisfy Eq. (12). Of course, the stability analysis does not take into account boundary conditions. For stability, gradient boundary conditions generally require the use of smaller  $\Delta t$  than predicted by Eq. (12).

For the case  $\alpha \neq 0$  and  $\beta \neq 0$ , herein denoted the mixed preconditioner, the stability analysis indicates that the method is conditionally stable, subject to the two conditions

$$\Delta t < \frac{1}{\pi} \sqrt{\beta^2 - \alpha} \quad (13)$$

and

$$\Delta t < \sqrt{\frac{\alpha f^2}{\frac{1}{\Delta x^2} + \frac{1}{\Delta y^2} - \frac{\omega^2}{4}} + \left( \frac{\beta \pi f^2}{\frac{1}{\Delta x^2} + \frac{1}{\Delta y^2} - \frac{\omega^2}{4}} \right)^2} \quad (14)$$

Generally, the second squared term on the right side of (14) is much smaller than the first term. For a typical scenario ( $\Delta x = 0.05, \Delta y = 0.1, f = 1, \alpha = 0.95, \beta = 1$ ),  $\Delta t < 0.071$  from Eq. (13) and  $\Delta t < 0.044$  from

Eq. (14). Consequently, the stability criteria yield  $\Delta t < 0.044$  in this mixed case example.

## NUMERICAL EXAMPLES

Let a plane wave propagate from the left into a semi infinite quiescent duct. The potential field is to be computed in the duct for  $0 < x < 1$ . Examples 1 to 3 illustrate the effects of changing  $\alpha$  and  $\beta$  with dimensionless frequency  $f = 1$  on the grid specified by  $\Delta x = 0.05$  and  $\Delta y = 0.5$ . Example 4 shows the effect of increasing the frequency, by using  $f = 5$ .

Because boundary conditions can introduce instabilities (Baumeister, 1982 and Cabelli, 1982) into otherwise stable finite difference schemes, it is important to test the iteration scheme for convergence in the absence of an exit boundary condition. Therefore, in these examples, the computational boundary is set at  $x = 50$ , far enough away from the true boundary  $x = 1$  that any artifacts arising from the exit boundary condition do not affect the solution in  $0 < x < 1$ .

The numerical results for plane wave propagation are compared to the exact results of the steady state solution, given by

$$\psi(x) = e^{i\omega x} \quad (15)$$

In the region  $0 < x < 1$ , the  $L_1$  norm of the global error  $e_k$  between the exact solution  $\psi$  and the numerical solution  $\phi^k$  at time step  $k$  is used as a measure of the convergence. The error is defined as

$$e_k = \int_0^1 \int_0^1 \sqrt{(\phi^k - \psi)(\phi^k - \psi)} dy dx. \quad (16)$$

**Example 1. Parabolic Preconditioning— $\alpha = 0, \beta = 1, f = 1$ .**

The choice of  $\alpha = 0$  eliminates the second order time derivative. The time increment  $\Delta t$  is set at 0.007. The maximum stable value, from Eq. (12), is 0.00797. The numerical and exact solutions are compared in Fig. 2(a) (real and imaginary parts of the potential) and in Fig. 2(b) (magnitude of the potential) after 1000 iterations. The numerical solution shows excellent agreement with the analytic solution. The error as a function of the iteration number is shown in Fig. 3. After 1000 iterations,  $e_{1000} = 0.0171$ . This residual error is the result of the usual round off and truncation errors associated with finite differences.

**Example 2. Mixed Preconditioning— $\alpha = 0.95, \beta = 1, f = 1$ .**

The time increment  $\Delta t$  is set at 0.04. The maximum stable value, from Eq. (14), is 0.049. The error as a function of the iteration number is shown in Fig. 4. After 100 iterations, the error is  $e_{100} = 0.0136201$ . It is important to note that the number of iterations required for convergence drops by an order of magnitude with mixed preconditioning as compared to parabolic preconditioning (shown by dashed line in Fig. 4). Therefore, a calculation which took 1 minute with the parabolic approach would now take only 6 seconds with the Hyperbolic Approach. Again, the numerical solution shows excellent agreement with the analytic solution after 100 iterations. The plots of the magnitude and the real and imaginary parts of the potential are virtually identical to Figs. 2(a) and (b), and hence are omitted. Clearly, mixed preconditioning is superior to

parabolic preconditioning because the number of iterations required for convergence is an order of magnitude lower.

**Example 3. Mixed Preconditioning— $\alpha = 16, \beta = 4.25, f = 1$ .**

The time increment  $\Delta t$  is set at 0.2. The maximum stable value, from Eq. (14), is 0.201. The error as a function of the number of iterations is shown in Fig. 5. After 500 iterations,  $e_{500} = 0.0136225$ . The results here are nearly identical to those shown in Fig. 4. The numerical solution again shows excellent agreement with the analytic solution. As before, the plots of magnitude and phase are omitted because they are virtually identical to Figs. 2(a) and (b). In this example, with the introduction of the large acceleration parameters, the time variable loses its physical meaning. In effect, the large  $\alpha$  reduces the effective speed of propagation  $C$  in Eq. (1) which then requires a longer time for the transient  $\phi$  to approximate the steady state solution  $\psi$  as required by Eq. (8). However, the critical parameter is the number of iterations required to obtain a solution. The convergence rates for examples 2 and 3 are nearly identical.

**Example 4. Mixed Preconditioning— $\alpha = 0.95, \beta = 1, f = 5$ .**

To resolve the shorter wavelengths associated with the higher frequency  $f = 5$ ,  $\Delta x$  is reduced by a factor of 5 to 0.01. The time increment  $\Delta t$  is set at 0.04. The maximum stable value, from Eq. (14), is 0.0497. The numerical and exact solutions are compared in Fig. 6(a) (real and imaginary parts of the potential) and in Fig. 6(b) (magnitude of the potential) after 1000 iterations. The numerical solution again shows excellent agreement with the analytic solution. The error as a function of iteration number is shown in Fig. 7. After 1000 iterations,  $e_{1000} = 0.0659$ . This error is about 5 times higher than that for the  $f = 1$  case. Since the two solution plots show roughly the same degree of accuracy, the change in total global error is apparently caused by the fact that there are 5 times as many grid points in the  $f = 5$  case. The number of grid points is proportional to the number of axial wavelengths or frequency. So dividing by the frequency gives a rough measure of the local error at each grid point, which is, in this case,

$$e_{k\lambda} = \frac{e_k}{f} = 0.0132 \quad (17)$$

It should be noted that acceptable solutions can be obtained using fewer iterations than the asymptotic values indicated by Figs. 7 to 9.

### Optimal Acceleration Parameters

Numerous numerical calculations were performed to determine the optimal choice of  $\alpha$  and  $\beta$  to reduce the number of iterations to convergence. In these calculations  $\alpha$  was set to 1 and  $\beta$  varied. Other choices of  $\alpha$  yield approximately the same rate of convergence. For convergence with minimum iterations, the time increment  $\Delta t$  and  $\beta$  were set as follows:

$$\Delta t_{opt} = \sqrt{\frac{\alpha f^2}{\frac{1}{\Delta x^2} + \frac{1}{\Delta y^2} - \frac{\omega^2}{4}}} \quad (18)$$

$$\beta_{\text{opt}} = \sqrt{\alpha + \pi^2 \Delta t_{\text{opt}}^2} \quad (19)$$

For  $\alpha = 1$ ,  $\Delta x = 0.05$ ,  $\Delta y = 0.5$  and  $f = 1$ , the optimal time increment  $\Delta t_{\text{opt}}$  from (18), is 0.0503. The optimal  $\beta_{\text{opt}}$  is calculated to be 1.01244 from Eq. (19). The error as a function of the number of iterations is shown in Fig. 8. After 100 iterations,  $e_{100} = 0.0137$ . The converged error is nearly identical to the  $\alpha = 0.95$  and  $\beta = 1.0$  nonoptimal case shown in Fig. 4. However, the optimal case reaches this error with nearly one order of magnitude in fewer iterations. Also, the error curve is seen to be much smoother. Therefore, a calculation which took 1 minute with the parabolic approach would now take only 1.8 seconds with the Hyperbolic Approach. The numerical solution again shows excellent agreement with the analytic solution. As before, the plots of magnitude and phase are omitted because they are virtually identical to Figs. 2(a) and (b).

The number of iterations to obtain the final solution can be reduced even further by increasing the spatial distance between nodes. For  $\alpha = 1$ ,  $\Delta x = 0.0833$  (66% increase),  $\Delta y = 0.5$  and  $f = 1$ , the optimal time increment  $\Delta t_{\text{opt}}$  from (18) is 0.0851. The optimal  $\beta_{\text{opt}}$  is calculated to be 1.03614 from Eq. (19) with a 1.001 factor of safety. The error as a function of the number of iterations is shown in Fig. 9. After 100 iterations,  $e_{100} = 0.0398$  which is approximately 3 times larger than the previous case shown in Fig. 8 with  $\Delta x = 0.05$ . However, this error is still acceptable for accurate solutions. In fact, after 16 iterations, the error level has dropped to 0.04732 which gives excellent results for phase and magnitude plots of the potential as shown in Figs. 10(a) and (b).

The speed at which the transient solution approaches the steady state Helmholtz solution is now discussed.

### Speed of Propagation

For the conventional wave equation, Pearson (1953) has shown that the total time  $t_T$  required for the steady state solution (15) to become established in the duct is equal to the time for a plane wave propagating at the speed of sound to reach the end of the duct. Similarly, with the preconditioned Helmholtz Eq. (9) and  $\alpha = 1$ , the steady state solution  $\psi(x)$  to the Helmholtz equation propagates outward at the dimensionless speed  $C$ , where from Eq. (2)

$$C = \frac{1}{f} = \frac{C_o^\#}{f^\# D^\#} \quad (20)$$

For a frequency  $f = 1$ , Fig. 11(a) shows the developing wave front (real and imaginary parts) as a function of the iteration number while Fig. 11(b) shows the magnitude of the potential. For this case,

$$t = \frac{L}{C} = Lf = 1 \cdot 1 = 1 \quad (21)$$

As seen in Fig. 11, the solution moves to the right with a distinct front at the speed  $C = 1$ . The front arrives at the exit at  $t \approx 1.0$ .

Similarly, for a frequency  $f = 5$ , Fig. 12(a) shows the developing wave front (real and imaginary parts) as a function of the iteration number while Fig. 12(b) shows the magnitude of the potential. For this case,

$$t = \frac{L}{C} = Lf = 1 \cdot 5 = 5 \quad (22)$$

As seen in Fig. 12, the solution moves to the right with a distinct front at the speed  $C = 0.2$ . The front arrives at the exit at  $t \approx 5.0$ .

The number of axial grid points and the number of iterations required for convergence are both directly proportional to frequency. A comparison of Figs. 11 and 12 shows the factor of 5 difference in the number of required iterations when the frequency is increased by 5. For increased frequency, the solution moves more slowly to the right. Generally, the solution time should be increased by 30 percent over that predicted by Eqs. (21) or (22) for more accurate results.

### SOLUTION METHODS

With the approach developed in this paper, three different solution techniques are now available to solve the Helmholtz equation, as shown in Fig. 13. The Fourier transform approach in the right column, with finite differences or finite elements, results in a matrix equation. Because this matrix is not positive definite, matrix elimination solutions are generally employed, requiring extensive computer memory for high frequency propagation. The transient solution to the hyperbolic wave equation, shown in the left column, eliminates matrix storage requirements by iterating finite difference approximations to the steady state solution.

The third option, preconditioning using the mixed formulation ( $\alpha \neq 0$ ,  $\beta \neq 0$ ), is shown in the center column. This approach eliminates matrix storage requirements, and has less stringent stability conditions than the transient solution, so it converges in fewer iterations.

### CONCLUSION

Accelerated numerical preconditioning of the Helmholtz equation has been developed. The field is iterated in time from an initial value of 0 to attain the steady state solution. The method eliminates the large matrix storage requirements of steady state finite difference or finite element techniques in the frequency domain. In each example provided, the numerical solution quickly and accurately converges to the exact steady state solution. The hyperbolic preconditioning developed in this paper has more than an order of magnitude faster convergence than the previously developed parabolic preconditioning approach.

### REFERENCES

- Baumeister, K.J., 1980, "Time-Dependent Difference Theory for Noise Propagation in a Two-Dimensional Duct," AIAA Journal Vol. 18, No. 12, pp. 1470.
- Baumeister, K.J., 1982, "Influence of exit impedance on finite difference solutions of transient acoustic mode propagation in ducts," ASME Journal of Engineering for Industry 104, pp. 113-120.
- Baumeister, K.J. and Kreider, K.L., 1996 "Finite Difference Time Marching in the Frequency Domain: A Parabolic Formulation for the Convective Wave Equation," ASME Journal of Vibration and Acoustics, Vol. 118, pp. 622-629.

Bayliss, A., Goldstein, C.I. and Turkel, E., 1983, "An Iterative Method for the Helmholtz Equation," *Journal of Computational Physics*, Vol. 49, pp. 443-457.

Cabelli, A., 1982, "Duct acoustics—A time dependent difference approach for steady state solutions," *J. Sound & Vibrations* 85, pp. 423-434.

Pearson, J.D., 1953, "The Transient Motion of Sound Waves in Tubes," *Journal of Mechanics and Applied Mathematics*, Vol. VI, Pt. 3, pp. 313-335.

Turkel, E., 1982, "Progress in Computational Physics," ICASE Report No. 82-23.

Turkel, E. and Arnone, A., 1993, "Pseudo-Compressibility Methods for the Incompressible Flow Equations," *Proceedings 11th AIAA Computational Fluid Dynamics Conference*, pp. 349-357, AIAA Paper 93-3329.

Turkel, E., Fiterman, A. and van Leer, B., 1994, "Preconditioning and the Limit to the Compressible to the Incompressible Flow Equations for Finite Difference Schemes," *Computing The Future: Advances and Prospects for Computational Aerodynamics*, M. Hafez and D.A. Caughey, eds., John Wiley and Sons, New York.

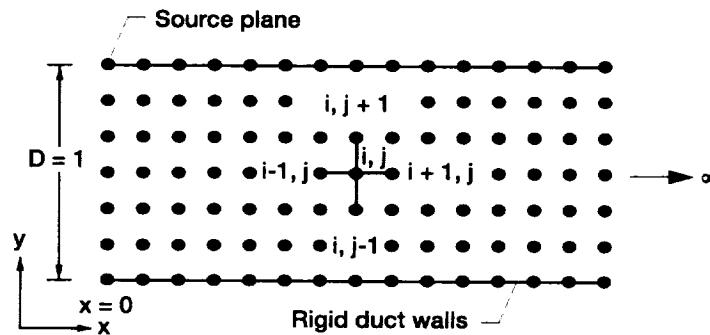


Figure 1.—Structured finite difference-time dependent (FD-TD) mesh for semi-infinite rectangular duct.

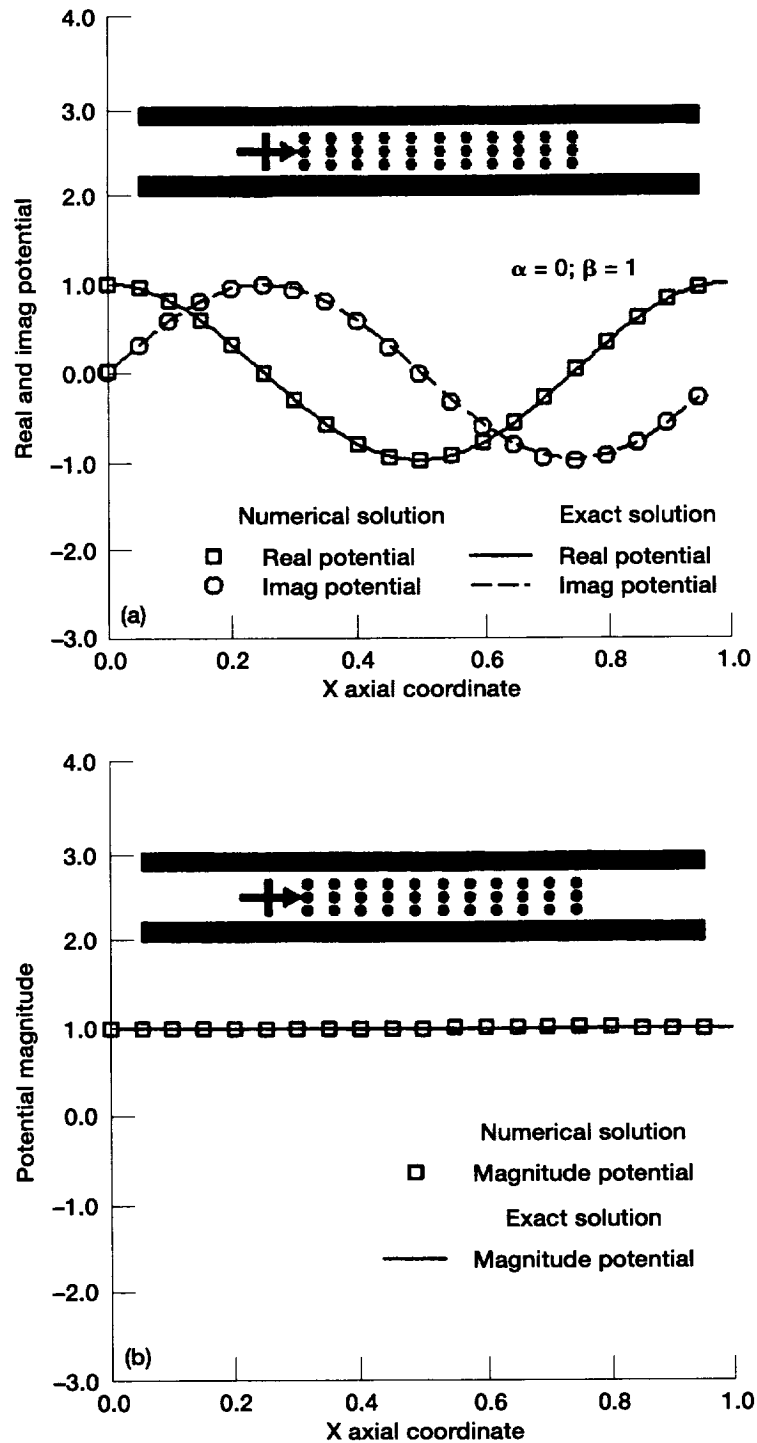


Figure 2.—Analytical and numerical potential profile along wall for plane wave propagating in a semi-infinite hard walled duct ( $f = 1$ ). (a) Real and imaginary parts. (b) Magnitude.

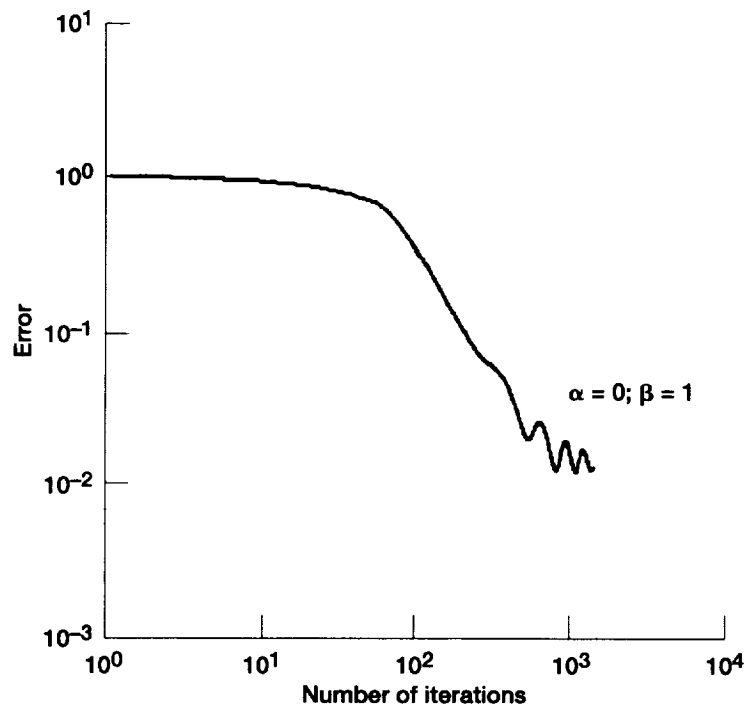


Figure 3.—Integrated solution error as a function of the number of iterations of the finite difference equations ( $f = 1$ ) → parabolic approximation.

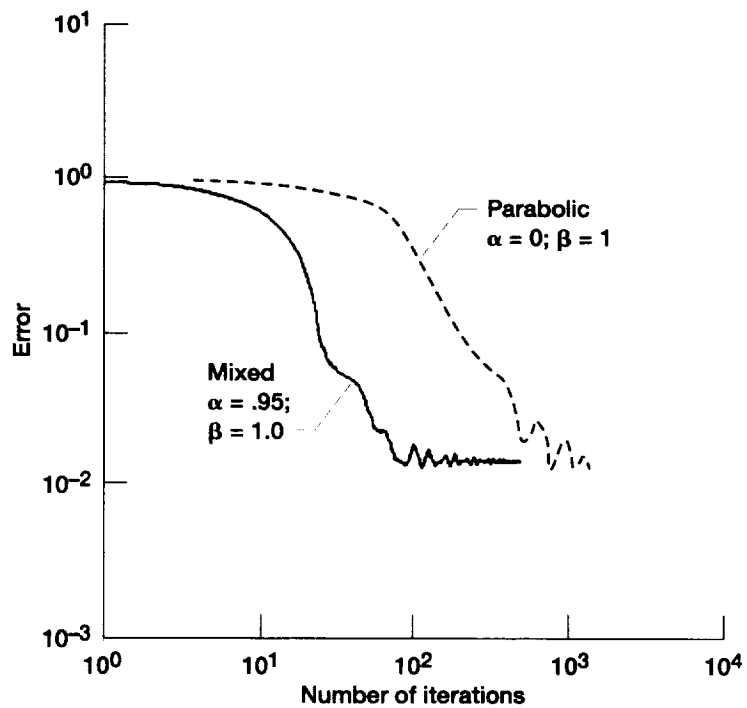


Figure 4.—Integrated solution error as a function of the number of iterations of the finite difference equations ( $f = 1$ ).

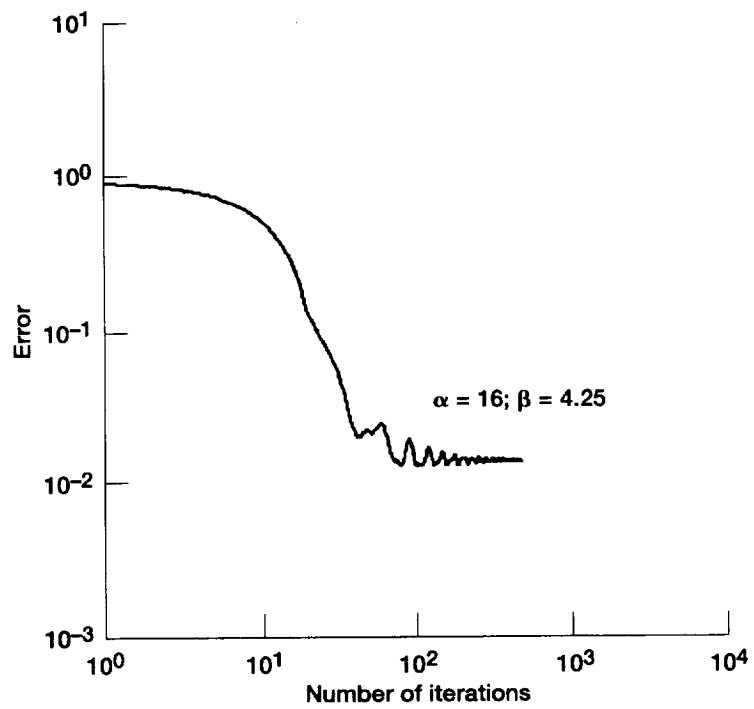


Figure 5.—Integrated solution error as a function of the number of iterations of the finite difference equations ( $f = 1$ ).

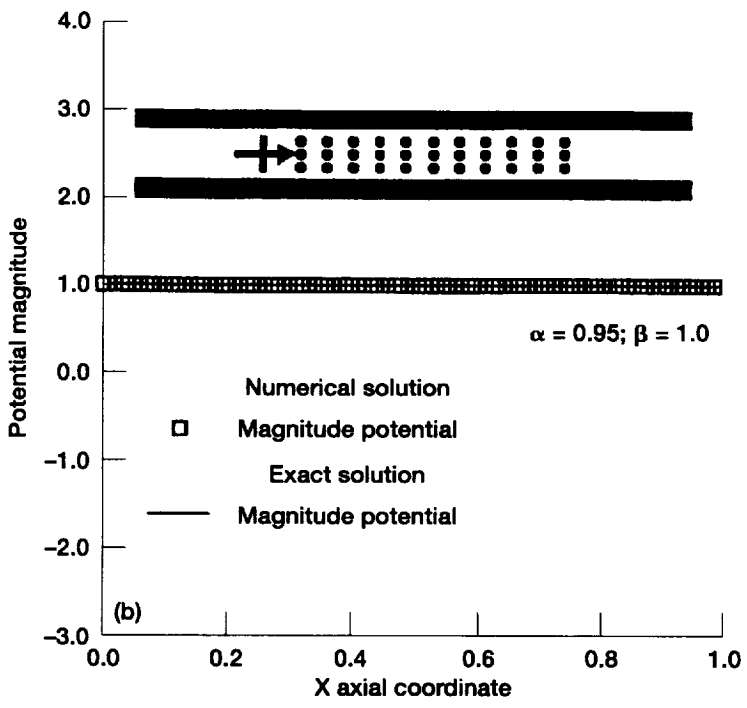
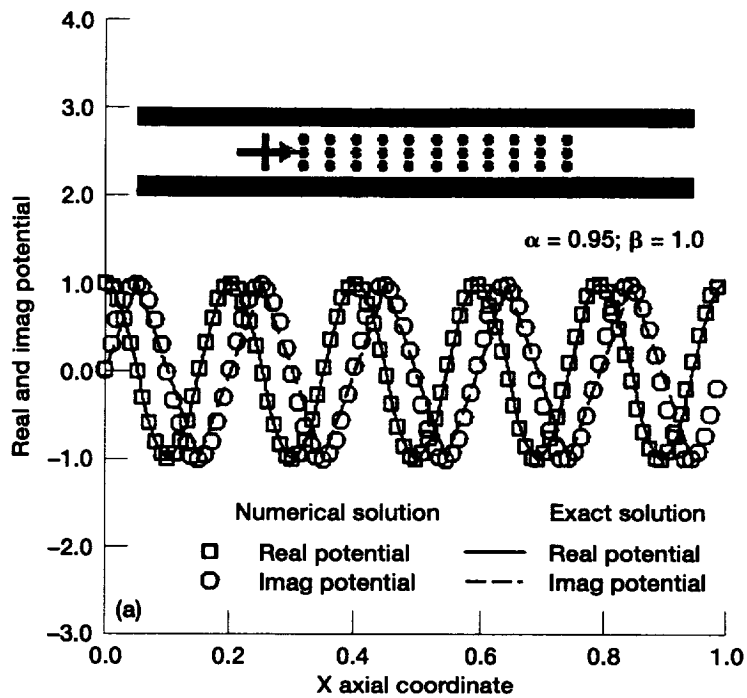


Figure 6.—Analytical and numerical potential profile along wall for plane wave propagating in a semi-infinite hard walled duct ( $f = 5$ ). (a) Real and imaginary parts. (b) Magnitude.

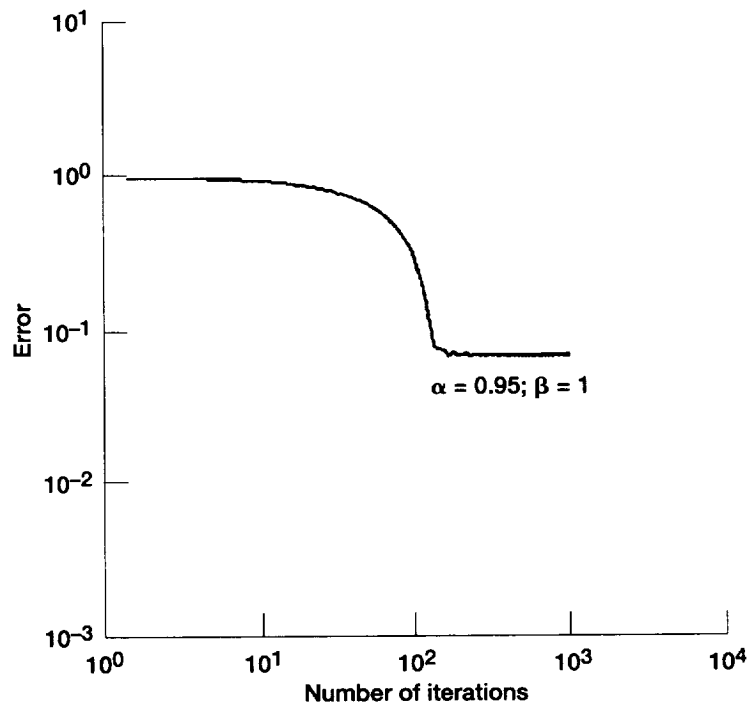


Figure 7.—Integrated solution error as a function of the number of iterations of the finite difference equations ( $f = 5$ ).

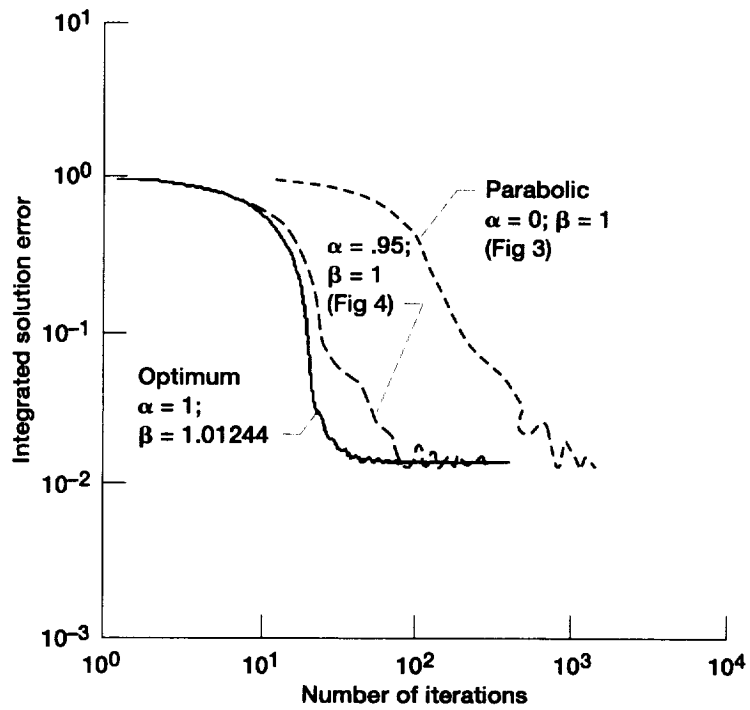


Figure 8.—Integrated solution error as a function of the number of iterations of the finite difference equations ( $f = 1$ ) with optimal parameters.

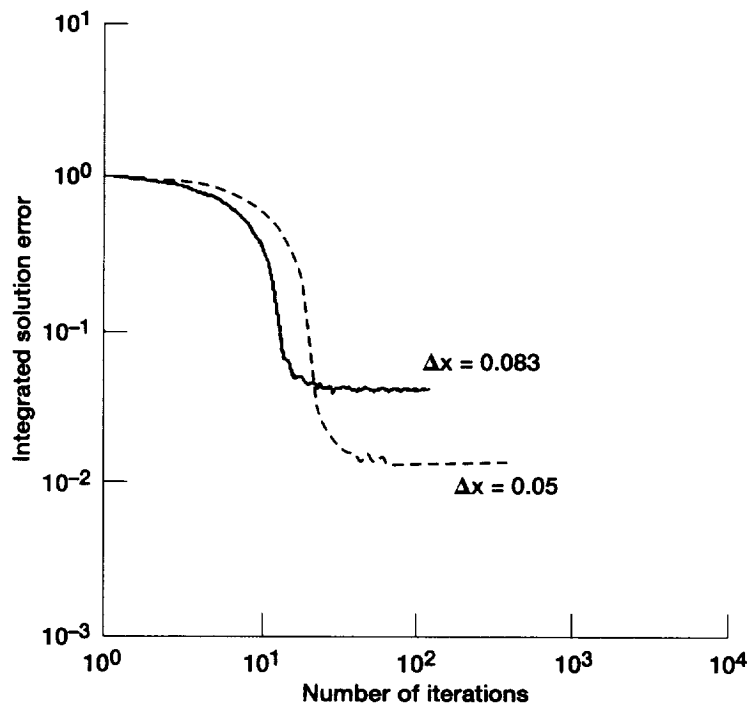


Figure 9.—Integrated solution error as a function of the number of iterations of the finite difference equations ( $f = 1$ ).

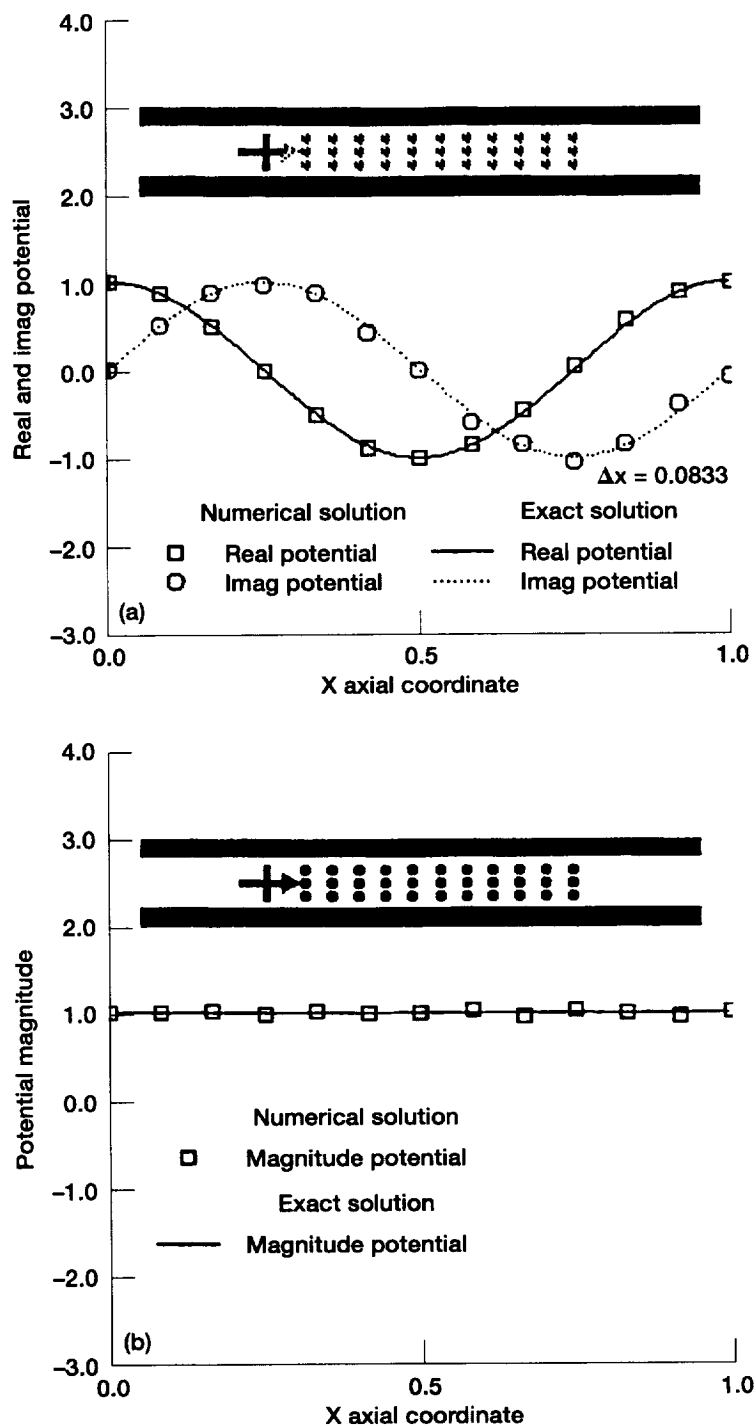


Figure 10.—Analytical and numerical potential profile along wall for plane wave propagating in a semi-infinite hard walled duct ( $f = 1$ ). (a) Real and imaginary parts. (b) Magnitude.

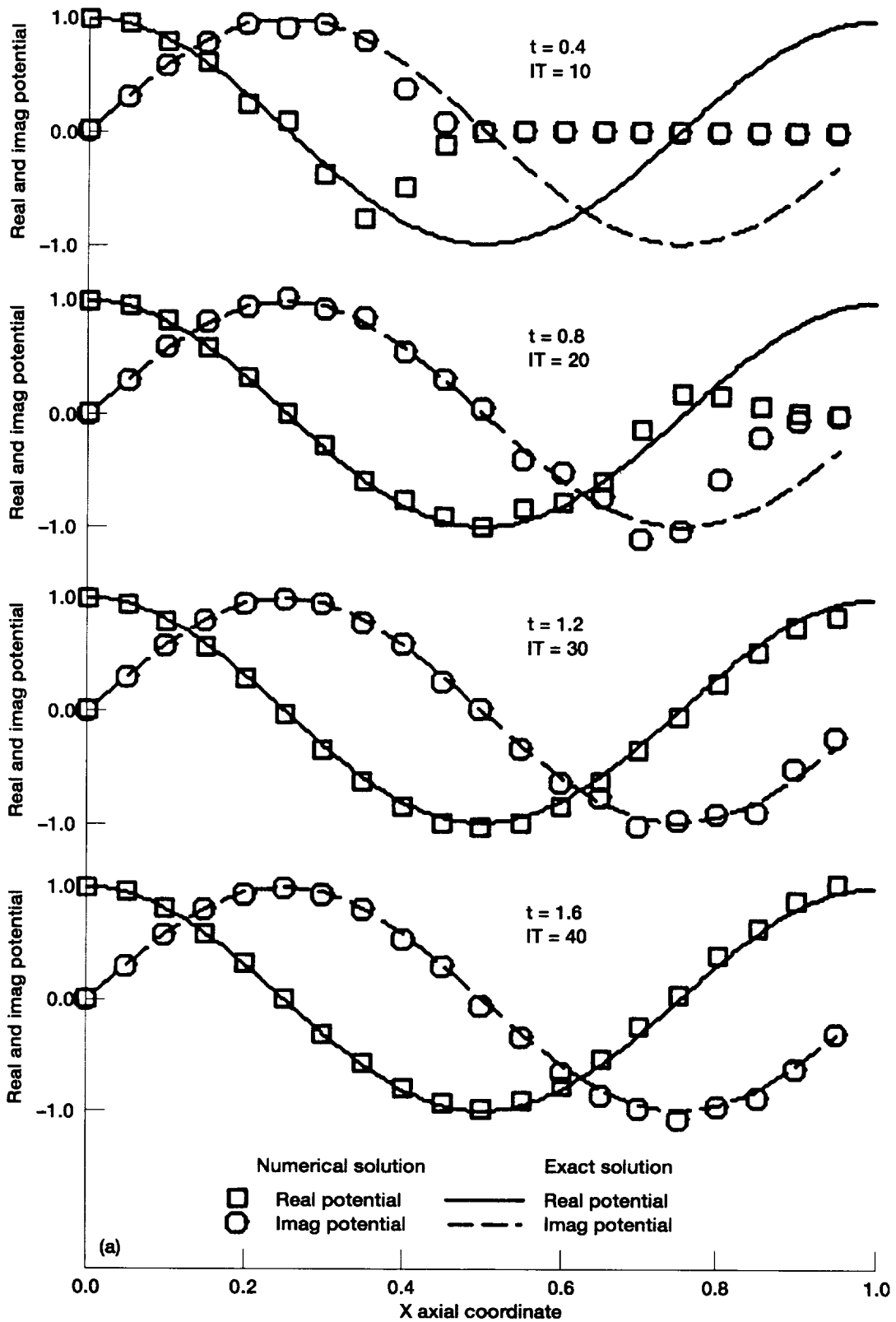


Figure 11.—Developing history of disturbance propagation in Fourier transformed domain as a function of number of iterations and time ( $f = 1$ ). (a) Real and imaginary parts. (b) Magnitude.

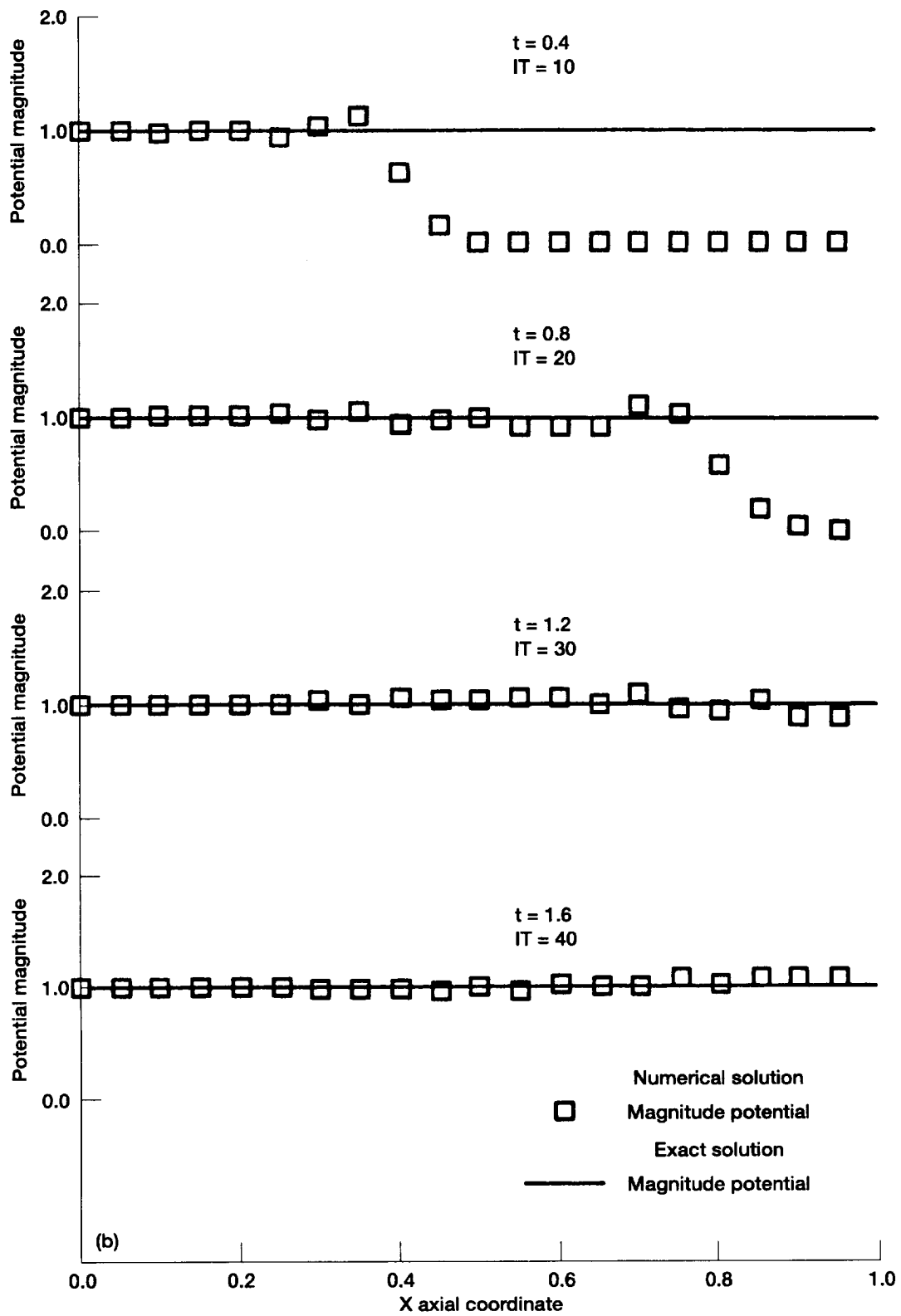


Figure 11.—Concluded. (b) Magnitude.

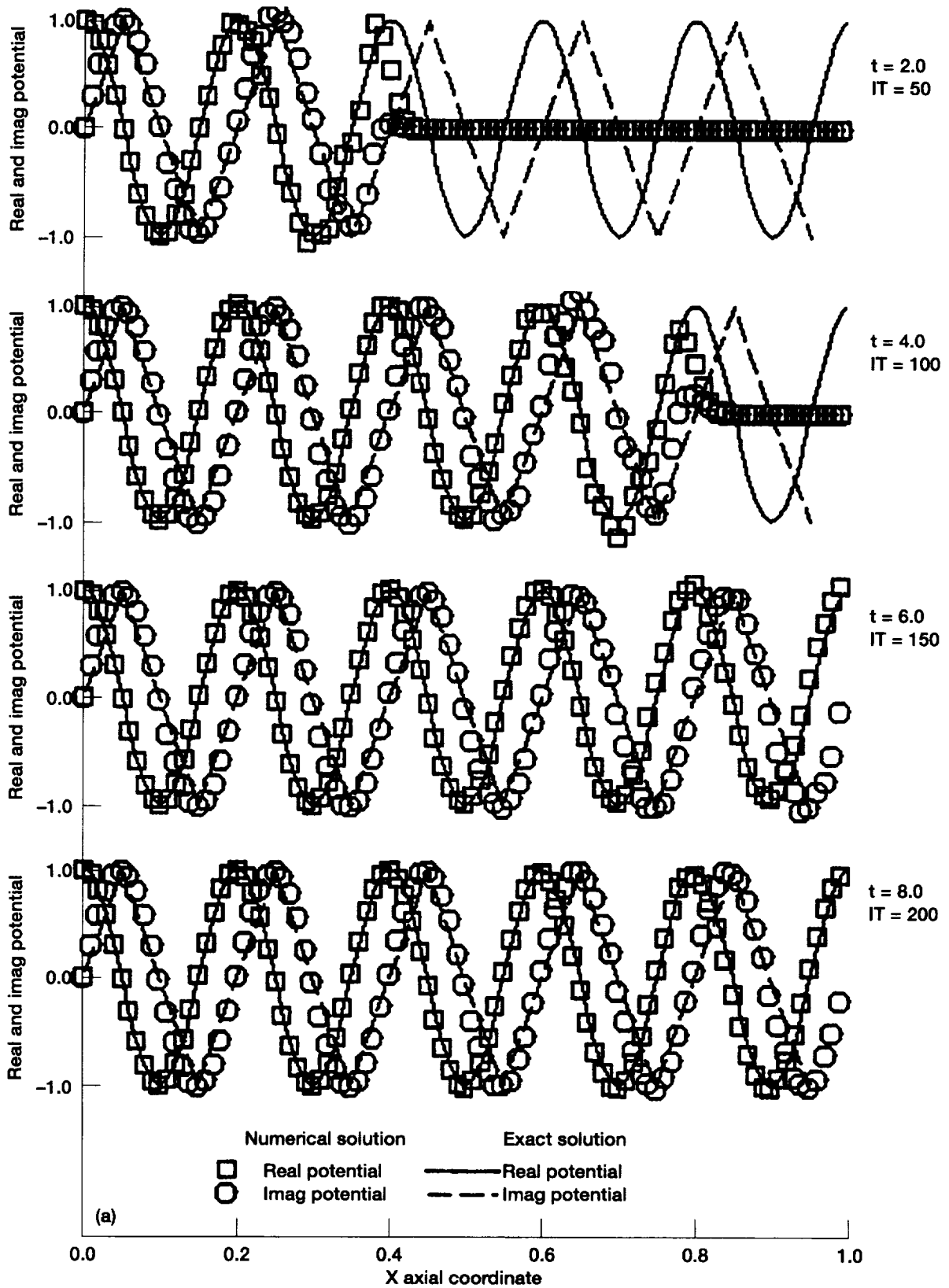


Figure 12.—Developing history of disturbance propagation in Fourier transformed domain as a function of number of iterations and time ( $f = 5$ ). (a) Real and imaginary parts. (b) Magnitude.

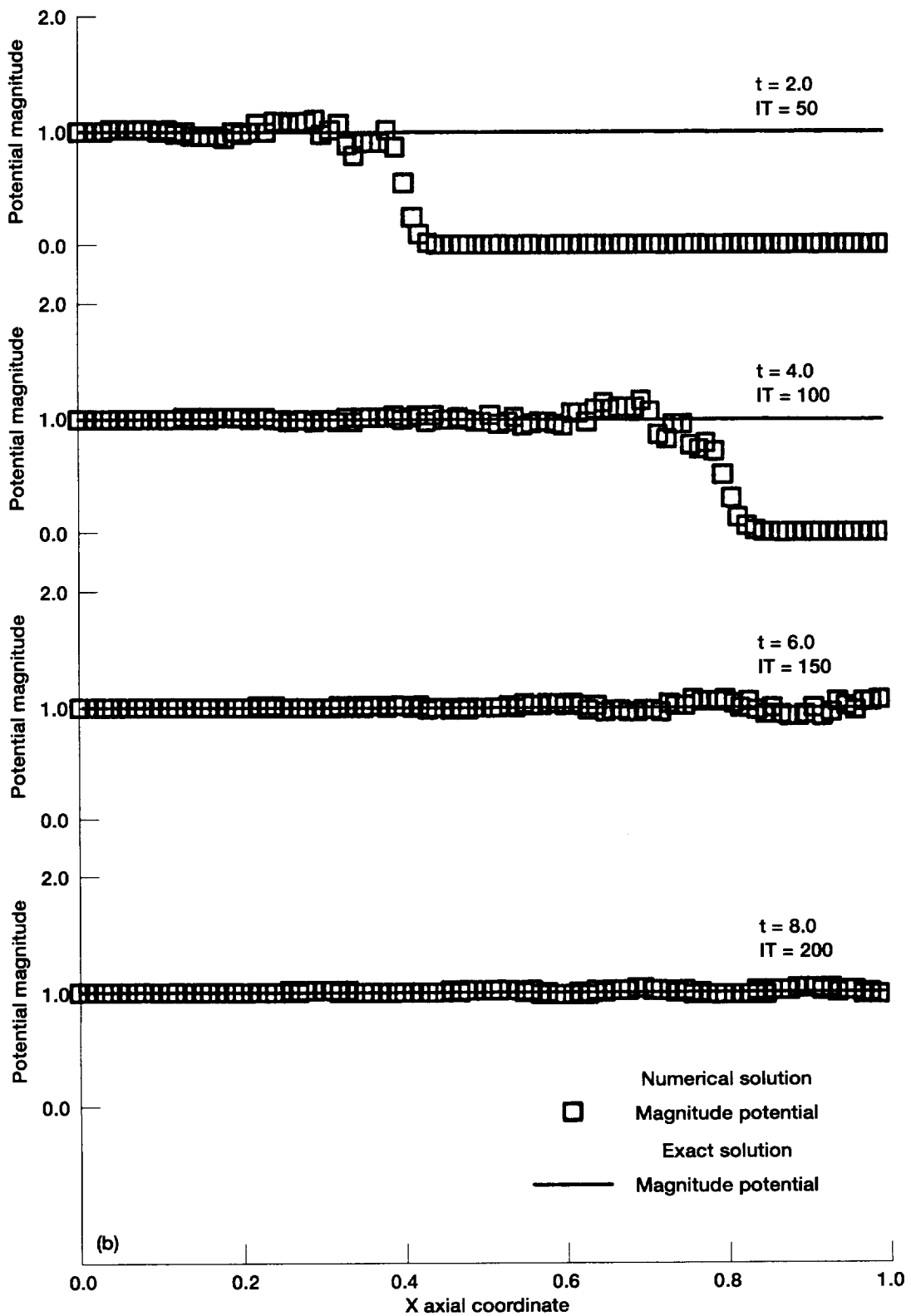


Figure 12.—Concluded. (b) Magnitude.

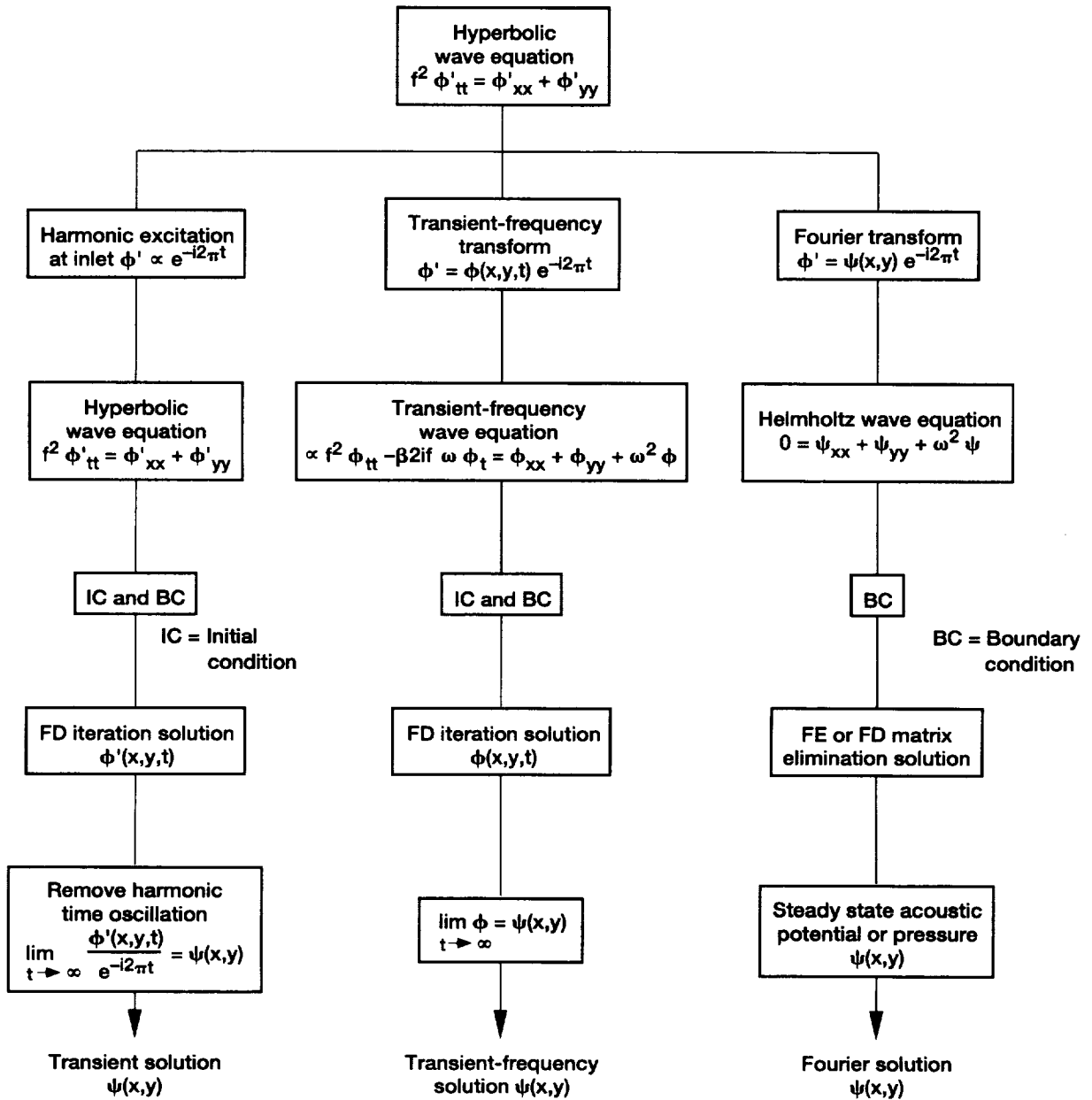


Figure 13.—Alternate finite difference/element methods in solving wave equations.



# REPORT DOCUMENTATION PAGE

*Form Approved*  
*OMB No. 0704-0188*

Public reporting burden for this collection of information is estimated to average 1 hour per response, including the time for reviewing instructions, searching existing data sources, gathering and maintaining the data needed, and completing and reviewing the collection of information. Send comments regarding this burden estimate or any other aspect of this collection of information, including suggestions for reducing this burden, to Washington Headquarters Services, Directorate for Information Operations and Reports, 1215 Jefferson Davis Highway, Suite 1204, Arlington, VA 22202-4302, and to the Office of Management and Budget, Paperwork Reduction Project (0704-0188), Washington, DC 20503.

<b>1. AGENCY USE ONLY (Leave blank)</b>		<b>2. REPORT DATE</b> March 1998	<b>3. REPORT TYPE AND DATES COVERED</b> Technical Memorandum	
<b>4. TITLE AND SUBTITLE</b>  Preconditioning the Helmholtz Equation for Rigid Ducts			<b>5. FUNDING NUMBERS</b>  WU-505-62-52-00	
<b>6. AUTHOR(S)</b>  Kenneth J. Baumeister and Kevin L. Kreider				
<b>7. PERFORMING ORGANIZATION NAME(S) AND ADDRESS(ES)</b>  National Aeronautics and Space Administration Lewis Research Center Cleveland, Ohio 44135-3191			<b>8. PERFORMING ORGANIZATION REPORT NUMBER</b>  E-10501	
<b>9. SPONSORING/MONITORING AGENCY NAME(S) AND ADDRESS(ES)</b>  National Aeronautics and Space Administration Washington, DC 20546-0001			<b>10. SPONSORING/MONITORING AGENCY REPORT NUMBER</b>  NASA TM-107349	
<b>11. SUPPLEMENTARY NOTES</b>  Responsible person, Dennis L. Huff, organization code 2200, (216) 433-3913.				
<b>12a. DISTRIBUTION/AVAILABILITY STATEMENT</b>  Unclassified - Unlimited Subject Category: 71  This publication is available from the NASA Center for AeroSpace Information, (301) 621-0390.			<b>12b. DISTRIBUTION CODE</b>  Distribution: Nonstandard	
<b>13. ABSTRACT (Maximum 200 words)</b>  An innovative hyperbolic preconditioning technique is developed for the numerical solution of the Helmholtz equation which governs acoustic propagation in ducts. Two pseudo-time parameters are used to produce an explicit iterative finite difference scheme. This scheme eliminates the large matrix storage requirements normally associated with numerical solutions to the Helmholtz equation. The solution procedure is very fast when compared to other transient and steady methods. Optimization and an error analysis of the preconditioning factors are present. For validation, the method is applied to sound propagation in a 2D semi-infinite hard wall duct.				
<b>14. SUBJECT TERMS</b>  Acoustics; Propagation; Ducts			<b>15. NUMBER OF PAGES</b> 24	
			<b>16. PRICE CODE</b> A03	
<b>17. SECURITY CLASSIFICATION OF REPORT</b> Unclassified	<b>18. SECURITY CLASSIFICATION OF THIS PAGE</b> Unclassified	<b>19. SECURITY CLASSIFICATION OF ABSTRACT</b> Unclassified	<b>20. LIMITATION OF ABSTRACT</b>	